Title
Design and implementation of fluidic micro-pulleys for flow control on centrifugal microfluidic platforms

Journal
Microfluidics and Nanofluidics, 16(6)

ISSN
1613-4982

Authors
Soroori, Salar
Kulinsky, Lawrence
Kido, Horacio
et al.

Publication Date
2014-06-01

DOI
10.1007/s10404-013-1277-7

Peer reviewed

Published in final edited form as:
Microfluid Nanofluidics. 2014 June ; 16(6): 1117–1129. doi:10.1007/s10404-013-1277-7.

Design and implementation of fluidic micro-pulleys for flow control on centrifugal microfluidic platforms

Salar Soroori[1,*], **Lawrence Kulinsky**[2], **Horacio Kido**[2,3], and **Marc Madou**[1,2,4]

[1]Department of Biomedical Engineering, University of California, Irvine, CA, 92697, USA

[2]Department of Mechanical & Aerospace Engineering, University of California, Irvine, CA, 92697, USA

[3]RotaPrep, Inc., Tustin, CA, 92782, USA

[4]UNIST, World Class University (WCU), Ulsan, South Korea

Abstract

Microfluidic discs have been employed in a variety of applications for chemical analyses and biological diagnostics. These platforms offer a sophisticated fluidic toolbox, necessary to perform processes that involve sample preparation, purification, analysis, and detection. However, one of the weaknesses of such systems is the uni-directional movement of fluid from the disc center to its periphery due to the uni-directionality of the propelling centrifugal force. Here we demonstrate a mechanism for fluid movement from the periphery of a hydrophobic disc toward its center that does not rely on the energy supplied by any peripheral equipment. This method utilizes a ventless fluidic network that connects a column of working fluid to a sample fluid. As the working fluid is pushed by the centrifugal force to move toward the periphery of the disc, the sample fluid is pulled up toward the center of the disc analogous to a physical pulley where two weights are connected by a rope passed through a block. The ventless network is analogous to the rope in the pulley. As the working fluid descends, it creates a negative pressure that pulls the sample fluid up. The sample and working fluids do not come into direct contact and it allows the freedom to select a working fluid with physical properties markedly different from those of the sample. This article provides a demonstration of the “micro-pulley” on a disc, discusses underlying physical phenomena, provides design guidelines for fabrication of micro-pulleys on discs, and outlines a vision for future micro-pulley applications.

Keywords

Hydrophobic fluidics; centrifugal microfluidics; micro-pulley; siphon; inward flow; pressure change

[*]Corresponding author: ssoroori@uci.edu, Tel. +1-949-824-1225.

1. Introduction

The field of centrifugal microfluidics has greatly evolved since its birth about fifty years ago (Burtis et al. 1972; Kido et al. 2007; Kirby et al. 2012; Gorkin et al. 2012a). Many functional techniques for processing chemical and biological samples and controlling fluid flow (such as valving, lysing, mixing, separation/clarification, metering, volume definition, and heating/cooling) have been developed to integrate biological/chemical assays onto these micro devices (Steigert et al. 2006; Cho et al. 2007; Mark et al. 2012). These efforts have led to the creation of integrated platforms that are called “Lab-on-disc” (Madou et al. 2006) in contrast to stationary “Lab-on-chip” platforms. Both Lab-on-disc platforms and Lab-on-chip devices share a common goal to function as fully automated and integrated sample-to-answer devices for chemical and biomedical applications, including biological assays (Madou et al. 2006; Ducree et al. 2007; Gorkin et al. 2010b).

One of the main differences between the disc-based and chip-based devices is the fluid propulsion mechanism. While Lab-on-chip devices rely mostly on external pressure to propel fluid through the system (even though capillary flow, electrowetting, and ferrofluids are getting more popular (Haeberle and Zengerle 2007; Love et al. 2004; Madou et al. 2006)), disc-based platforms rely on the forces that are generated due to spinning (mainly the centrifugal force). The uni-directional nature of the centrifugal force (from the center toward the outer edge of a spinning platform) has long presented a challenge of not being able to optimize the access to all the space available on a disc (Gorkin et al. 2012b; Gorkin et al. 2010a). For example, the short distance from the disc center to its edge presents a practical limitation on the complexity of the assays implemented on discs as assays with a large number of fluidic steps (involving separate reservoirs and fluidic conduits) do not fit into a limited space between the disc’s center and its edge. One way to bypass this space limitation is to re-route the fluid toward the disc center once it reaches the disc’s outer edge in order to continue the assay again from the disc’s center to its edge. Several different techniques have been developed so far to bring the fluid back toward the center of the disc. For example (Li et al. 2009; Garcia-Cordero et al. 2010) utilized the balance between the centrifugal and capillary forces to recirculate fluid in channels running radially from the center to the edge of the disc. Thermo-pneumatic pumping is another approach that has been demonstrated by (Abi-Samra et al. 2011; Thio et al. 2013) to direct liquid from a reservoir at the outer edge of the disc toward the center by heating air pockets in fluidic networks and using the pumping power generated by the air expansion. Also (Noroozi et al. 2011) demonstrated that the gas produced from electrolysis can be used to propel fluid inwardly on the disc. Another gas-driven inward fluid propulsion technique was demonstrated by (Kong and Salin 2010; Kazarine et al. 2012) that utilized pressurized air supplied by external gas containers.

The fluid transfer methods listed above can be separated into two broad categories: fluid transport caused by capillary forces and fluid propulsion that uses externally supplied energy (in the form of heat or electricity such as thermo-pneumatic, hydrolysis-based and active pressurized air pumping). Techniques that rely on the capillary force for liquid movement have two drawbacks: 1) while it is possible to move fluid up in the channel, it is very difficult to empty fluid from hydrophilic channels into the reservoir as the same capillary

force that causes propulsion will prevent emptying of the fluid from the reservoir; 2) hydrophilic surfaces guarantee propulsion of the fluid when the disc does not spin (i.e. there is no centrifugal force that counter balances the capillary force), thus the system is "normally on" – on a stationary disc, for example, the fluid advancement through the channels is driven by the capillary force until the disc is spun to generate the counter-acting centrifugal force. Therefore in situations that the spinning is disrupted (e.g. due to momentary motor power failure or low battery levels) unrestrained flow in the system is triggered. In contrast, in "normally off" systems the fluid stays in place until sufficient propulsion force is applied (controlled by setting specific angular velocities for spinning the disc) leading to more robust control of the fluid flow. In order for fluids to stay in the channel and not move in the absence of rotation, the disc material should be hydrophobic and we refer to microfluidics of the hydrophobic systems as "hydrophobic fluidics" (while study of the fluid transport in hydrophilic fluidic networks can be termed "hydrophilic fluidics"). Most of the plastics that are used to fabricate microfluidic discs with are inherently hydrophobic (Becker and Gärtner 2008; Tsao and DeVoe 2009) and thus an additional advantage of "hydrophobic fluidics" over "hydrophilic fluidics" is the absence of the surface treatment step required to make plastic surfaces more hydrophilic.

Fluid propulsion techniques based on thermo-pneumatic and pressurized air pumping and also electrolytic gas generation all require external equipment. Such equipment include infrared lamp (heat source) for thermo-pneumatic pumping, pressurized gas container for air pumping and electrodes/electrical hardware for electrolytic gas propulsion. Additional equipment increases the complexity and cost of the system (Gorkin et al. 2010b; Madou 2002).

Recently, various research groups have offered solutions for bringing fluids from the periphery of the disc toward the disc center without the use of capillary force or the need for peripheral equipment. For example (Zehnle et al. 2012) utilized the combination of air compression in ventless chambers and tuning the hydraulic resistance of connecting channels to propel fluid from the outer edge of the disc toward its center. In another approach (Gorkin et al. 2012b) proposed the use of negative pressure that is generated within on-disc radial channels as a fluid empties from them. This negative pressure pulls the fluid in an adjoining channel toward the disc center (albeit for a small distance). Another group demonstrated that the movement of a fluid from the center of a disc toward its edge can be used to push another fluid from the periphery of the disc closer to the center of the disc (Kong et al. 2011). In this method however, too little of the fluid can be raised toward the disc's center due to presence of a large dead volume.

In this paper we demonstrate a mechanism for fluid movement from the periphery of a hydrophobic disc toward its center that does not rely on energy supplied by peripheral equipment, but that utilizes potential energy of the working fluid that is stored in a reservoir on the disc and is coupled to working fluid through a ventless chamber. Thus when the working fluid is pushed by the centrifugal force to move toward the periphery of the disc, the sample fluid is pulled up toward the center of the disc analogous to a physical pulley where two weights are connected by a rope passed through a block. Thus we name this mechanism a micro-pulley. The connection between the movement of the column of

working fluid and the pull of the sample fluid is facilitated through a ventless network of channels and reservoirs. As the working fluid descends, it creates a negative pressure that pulls the sample up. Since the sample and working fluids do not come into direct contact, the working fluid can be selected with physical properties markedly different from those of the sample. We first outline the concept of how liquids can travel against the direction of the centrifugal force by only relying on the inherent properties of the spinning platforms. An analytical model that follows describes the physical framework underlying the fluidic operation on such a system. The analytical model is validated by the presented experimental data. We propose the design criteria to be used for creating such “micro-pulley” systems on spinning discs to affect the fluid transfer from the disc edge to its center. We conclude with an example of the proposed application for micro-pulley fluid transfer for executing complex multi-step assays in the Lab-on-disc format.

2. Concept

2.1 Flow mechanism

The fluid flow control mechanism presented in this study is based on utilizing the force and pressure gradients that are inherent to the spinning platforms. The direction of the centrifugal force vector is always directed radially outward from the center of the rotating system in the plane of the rotation. In order to move a volume of fluid from the outer edge toward the center, an opposing force should dominate the centrifugal force. The opposing force in this case is caused by the pressure drop that is generated by the exit of another fluid (we call it the working fluid) from a chamber that is connected to the sample fluid chamber (Figure 1a) The sample and working fluid chambers are connected through a ventless fluidic network that includes another reservoir (called the transfer chamber). The transfer chamber is designed to collect the sample fluid transferred from the sample fluid chamber positioned at the disc’s edge. The working fluid chamber is connected to the vented (i.e. opened to the atmosphere) waste chamber through a capillary valve that holds the working fluid in place until the disc rotates with high enough angular velocity to burst that capillary valve, starting the fluid transfer process.

After the capillary valve bursts and the working fluid starts to move into the waste chamber, the pressure within the fluidic network (connecting the sample and working fluid chambers) drops since now the gas in the ventless network occupies a larger volume. This pressure drop creates a pressure gradient between the atmospheric pressure above the fluid in the sample fluid chamber and sub-atmospheric pressure in the fluidic network, including the transfer fluid chamber. This pressure difference increases as more working fluid empties from the working fluid reservoir, eventually causing the movement of the sample fluid toward the disc center and into the sample transfer chamber (Figure 1b).

2.2 Micro-pulley analogy

The fluid flow mechanism described above is analogous to the way a simple pulley functions. The mass to be pulled up through the pulley is the sample fluid. The ventless network of channels and sample transfer reservoir that connects the working fluid and the sample fluid is analogous to the rope connecting two weights in the pulley (Figure 1c). The

force related to the pressure drop generated by the exit of the working fluid is analogous to the rope tension in the pulley analogy. The column of the working fluid in the micro-pulley analogy is represented by the heavier weight (or else by a pulling force in Figure 1c) that is connected via the "rope" to the lighter weight (the sample fluid column). As the working fluid column empties into the waste chamber its weight is reduced. One of the design criterions discussed below will ensure that the pulley can successfully operate to empty the sample reservoir completely into the transfer chamber before the column of the working fluid becomes too small to pull up the sample fluid.

The micro-pulley analogy further helps to explain some characteristic behaviors of the system. We have discovered that while the micro-pulley system works well for fluid transfer below a certain angular velocity, once the angular velocity is increased above roughly 2600 revolutions per minute (rpm) the fluid transfer does not happen anymore. As will be demonstrated below, that behavior is analogous to the pulley system where the weights are connected by an elastic rope. If the rope is elastic it has a limitation on the weights of the loads for the system to operate well; when this limit is exceeded the rope will stretch out and/or break. The weights of the loads (both, the sample column and the working fluid column) are proportional to the square of the angular velocity [evident, for example, from Equation (4) below]. When the increased angular velocity causes the weights of the liquid column to be higher than the maximum force supported by the connecting air column in the ventless network (i.e. the "rope") the micro-pulley does not function properly.

While the pulley system presents a powerful analogy for understanding of the underlying physics of the centrifugal microfluidic device described in this work, this analogy is not exact. The most significant difference in physics between the pulley and the fluidic system presented in this work is the magnitude and behavior of forces acting on the loads (i.e. on liquid columns). While for the physical pulley system the force acting on each load is nearly constant throughout the action of the pulley, for our system, forces acting on each column are dynamic – they are changing as each liquid column moves toward or away from disc's center; so the physical framework of the microfluidic system discussed in the next section, is more complex than that of the actual pulley.

3. Analytical model

In this section we present an analytical model that describes the underlying physics governed by the interplay of the centrifugal forces enacted on the columns of the sample fluid and of the working fluids as well as the pressure changes that occur within the trapped air pocket in the ventless connecting network.

3.1 The elasticity of the "rope" of the micro-pulley - air pressure changes within the ventless network

We will use P_1 to denote the initial pressure existing within the ventless network that connects the working fluid and the sample fluid. As the working fluid starts to exit from the working fluid reservoir into the waste chamber, the pressure in the ventless network changes to a new value P_2.

According to Boyle's law:

$$P_2 = P_1 \frac{V_1}{V_2} \quad (1)$$

When the working fluid chamber is completely filled $P_1 = P_{atm}$ (atmospheric pressure) and $V_1 = V_{mid}$ (the volume of the air trapped in the ventless space between the sample and working fluids). As soon as the working fluid starts to empty into the secondary reservoir the air pocket trapped in the ventless network expands to occupy volume V_2:

$$V_2 = V_{mid} + A_w \int_{R_1 - L}^{R_1 - R_0} dR = A_w \Delta L \quad (2)$$

where A_w is the working fluid chamber's cross-sectional area, L is the distance from the disc's center to the top of the working fluid level, R_0 and R_1 are the distances of the top and bottom of the working fluid chamber from the disc's center, respectively (see Figure 2). Hence:

$$P_2(L) = P_{neg} = P_{atm} \frac{V_{mid}}{V_{mid} + A_w \Delta L} \quad (3)$$

P_2 (L) is a sub-atmospheric pressure that is generated by empting the working fluid for a distance ΔL.

When the working fluid exits, but the sample fluid is not yet pulled up by the sub-atmospheric pressure in the ventless network (P_{neg}), the volume of the ventless network is increased further until one of the following happens: 1) pressure in the ventless network eventually becomes low enough to pull up the sample fluid, at which point the volume of the ventless network stays nearly constant and the movement of the working fluid causes the corresponding movement of the sample fluid, - i.e., the system starts to act as a pulley with a non-stretching rope (we will discuss the mechanics of this modality in the next section), or 2) the working fluid will empty completely from the reservoir before the sample fluid transfers to the upstream transfer chamber, - i.e. the pulley's rope failure. In our physical pulley analogy the latter behavior is similar to a pulley with heavy weights on both sides of the block and a rope that stretches out instead of transferring the momentum from one load to the other load across the block. The underlying physics of this microfluidic system is governed by the balance between the sub-atmospheric pressure within the ventless network that pulls the sample fluid up and the centrifugal force that pushes the column of the sample fluid down.

Equation (3) above describes the pressure in the ventless network, while the centrifugal pressure dP_ω acting on a fluidic element of height dr located at distance r away from the disc's center can be expressed in differential form as (Madou 2002):

$$dP_\omega = \rho \omega^2 r dr \quad (4)$$

where ρ is the density of the sample's liquid column and ω is the angular velocity of the rotating disc.

As the sample fluid level in the transfer channel rises the centrifugal pressure experienced by this fluid also increases. The transfer of the sample fluid to the transfer chamber is a dynamic process that involves the force/pressure balance between the negative pressure generated in the ventless transfer network, the centrifugal pressure that is experienced by both, the sample and working fluids, and the capillary force that in the case of a hydrophobic system (such as untreated plastic material of the disc) acts against the fluid advancement. Assuming laminar flow conditions in the fluidic transfer network (i.e. flow dominated by viscous effects) and neglecting the capillary forces, the force balance at the interface between the sample fluid and the air in the ventless chamber located at distance Δ*r* above the surface of the sample fluid in the sample fluid chamber (see Figure 2) is:

$$(P_{atm} - P_{neg}) \cdot A_{tr} = A_{tr} \cdot \rho\omega^2 \int_{r_1-\Delta r}^{r_1} r dr = A_{tr} \cdot \frac{\rho\omega^2}{2}[{r_1}^2 - (r_1 - \Delta r)^2] \quad (5)$$

where r_1 is the distance from center of the disc to the initial top level of the fluid in the sample chamber.

The downward force exercised by the column of sample fluid reaches its maximum value when the last drops of the sample fluid just empty from the sample reservoir. The balance of forces at this point is:

$$(P_{atm} - P_{neg}) \cdot A_{tr} = A_{tr} \cdot \frac{\rho\omega^2}{2}({r_2}^2 - {r_0}^2) \quad (6)$$

The maximum negative pressure [i.e. minimum ($P_{atm} - P_{neg}$) term] in Equation (6) can be calculated from Equation (3) above. Neglecting volume reduction of the ventless network due to the rise of the sample fluid, the maximum value of P_{neg} is achieved when the working fluid exits the working fluid reservoir completely (i.e. for $\Delta L = R_1 - R_0$):

$$P_{neg(max)} = P_{atm} \frac{V_{mid}}{V_{mid} + A_w \Delta L_{max}} = P_{atm} \frac{V_{mid}}{V_{mid} + A_w (R_1 - R_0)} \quad (7)$$

Hence, the expression for the maximum angular velocity of the disc above which the "micro-pulley" system does not work is given by:

$$\omega_{max} = \sqrt{\frac{2 \cdot P_{atm} \cdot A_w \cdot (R_1 - R_0)}{\rho \cdot ({r_2}^2 - {r_0}^2) \cdot (V_{mid} + A_w (R_1 - R_0))}} \quad (8)$$

where ρ is the density of the sample fluid. The value of the maximum angular velocity for specific details of the micro-pulley system is calculated in the section 4.3.

3.2 Mechanics of the fluid movement of the "micro-pulley" system on a disc

For angular velocities below ω_{max} presented above, the micro-pulley on a disc functions analogous to a physical pulley where the rope does transfer the forces between the two weights. In this section we will consider conditions (including the geometries of the working fluid and the sample fluid reservoirs, heights of the sample and the working fluid columns, densities of the sample and the working fluids) necessary to transfer the sample fluid upstream into the transfer reservoir. The physical principle is rather simple – the descending "heavier" working fluid column pulls up the "lighter" sample fluid column, transferring it into the upstream transfer reservoir. The complexity of the analysis is due to dependence of the force applied to a fluid element on the square of the angular velocity and the column's distance from the center of rotation. Therefore, the force balance between the working and the sample fluid columns continues to change during the movement of the corresponding fluids.

In order for the micro-pulley to successfully operate on a disc, the hydrostatic pressure head of the working fluid needs to be greater than the hydrostatic pressure head of the sample fluid in the transfer channel (see Figure 2):

$$\rho_{wk}\omega^2\int_{R_0+\Delta L}^{R_1} r dr > \rho_{sm}\omega^2\int_{r_1-\Delta r}^{r_1+\Delta H} r dr$$

or:

$$\rho_{wk}[{R_1}^2 - (R_0+\Delta L)^2] > \rho_{sm}[(r_1+\Delta H)^2 - (r_1-\Delta r)^2] \quad (9)$$

where Δr represents the rise of the sample fluid in the transfer channel above the initial level of the fluid (located at the distance r_1 from the disc's center) in the sample reservoir, ΔH represents the descent of the sample fluid in the sample reservoir relative to its initial level, ΔL is the distance the working fluid descends with respect to the top of the working fluid reservoir, and the subscripts *Wk* and *sm* refer to working fluid and sample fluid, respectively (see Figure 2). This analysis neglects the capillary resistance forces in the hydrophobic channels.

Due to incompressible nature of the liquid (and thus its volume conservation), there is a fixed relationship between ΔH, the change in the level of sample fluid in the sample fluid chamber of cross-sectional area A_{sm}, and Δr, the rise of the sample fluid in the transfer channel of the cross-sectional area A_{tr}:

$$\Delta H \cdot A_{sm} = \Delta r \cdot A_{tr}$$

Assuming the air pocket in the ventless network does not stretch further after the start of the fluid transfer, we can extend the volume conservation relationship to the liquid in the working reservoir of cross-sectional area A_w:

$$\Delta r=\Delta L\frac{A_w}{A_{tr}} \quad (10)$$

and

$$\Delta H=\Delta L\frac{A_w}{A_{sm}} \quad (11)$$

Therefore, we can re-write Inequality (9) as:

$$\rho_{wk}[{R_1}^2-(R_0+\Delta L)^2]>\rho_{sm}\left[(r_1+\Delta L\frac{A_w}{A_{sm}})^2-(r_1-\Delta L\frac{A_w}{A_{tr}})^2\right] \quad (12)$$

While the current section has outlined the general physical framework for operation of the micro-pulley on a disc, in the next section we will discuss the applications of the presented equations to establish the design criteria for successful implementation of the micro-pulley platforms on discs.

4. Design Criteria

In order to successfully operate the micro-pulley on a disc and pull the sample fluid toward the center emptying it into the transfer chamber, it is necessary to satisfy three sets of criteria: appropriate geometry of the working fluid chamber, sufficient volume of the fluid in the working chamber, and a suitable range of angular velocities.

4.1 Criterion for the geometry of the working fluid chamber

The overall length and position of the working fluid chamber affects the action of the micro-pulley in several ways: 1) the length of the chamber determines the maximum angular velocity for micro-pulley action as described in Equation (8) (note that the position and the length of the transfer channel also influence ω_{max}); 2) the hydrostatic pressure head of the working fluid at all times needs to be greater than the hydrostatic pressure head of the sample fluid as described by Inequality (12). This latter condition is especially important since the fluid transfer is a dynamic process where, while the hydrostatic pressure head of the working fluid is decreasing, the hydrostatic pressure head of the sample fluid is increasing to reach its maximum value of $\frac{\rho_{sm}\omega^2}{2}({r_2}^2-{r_0}^2)$ (see the discussion in section 3.1).

4.2 Criterion for the volume of the working fluid

The volume of the fluid in the working fluid chamber should be greater than the volume of the sample fluid to be transferred to the transfer reservoir. Section 6 below discusses that we see some additional stretching of the air pocket in the ventless network while the micro-pulley is in operation (some air diffusion into the air pocket is also possible), thus a safety margin in selection of the volume of working fluid is advisable.

4.3 Criterion for the angular velocity

The three main parameters affecting the window of angular velocities for successful operation of the micro-pulley on a disc are: the stretching of the air pocket in the ventless network that determines the maximum angular velocity to be used, the burst frequency of the hydrophobic passive valve at the working fluid chamber exit representing the minimum angular velocity to be used, and the density of the working fluid that affects the burst frequency of the capillary valves.

The theoretical value of the maximum angular velocity to be used in a micro-pulley on a disc is given by Equation (8) above. Substituting the values for the specific geometry of our microfluidic system (see Supplementary Materials), the maximum operating angular velocity was calculated to be 2600 rpm.

The working fluid chamber relies on a passive hydrophobic valve to hold the working fluid prior to initiation of the micro-pulley fluid transfer. The channel width at the chamber's exit affects the burst pressure of the valve (Madou et al. 2001; Grumann et al. 2005) given by the equation (Chen et al. 2008):

$$\Delta P_b = \frac{2\gamma_{la}}{w}\left[-\frac{w}{\text{âĎŐ}}\cos\theta_c - \cos(\theta_c+\beta)\right] \quad (13)$$

where γ_{la} is the surface tension of the working fluid, w is the width of the exit of the working fluid chamber, h is the depth of the working fluid chamber, θ_c is the contact angle of the working fluid with the walls of the disc, and β is the opening wedge angle of the valve channel that is taken to be 90° for current disc design.

The burst frequency of the capillary valve can be deduced from the equation describing the balance between the capillary forces at the exit of the working fluid chamber, the hydrostatic pressure head of the working fluid (we assume that the working fluid reservoir is filled completely), and the sub-atmospheric pressure in the ventless network that also acts against the exit of the working fluid:

$$\Delta P_b + (P_{atm} - P_{neg}) = \rho_{wk}\omega^2 \int_{R_0}^{R_1} r dr = \frac{\rho_{wk}\omega^2({R_1}^2 - {R_0}^2)}{2} \quad (14)$$

If the pressure in the ventless network is not significantly lower than the atmospheric pressure at the point where the valve bursts, the burst frequency for the capillary valve is given by:

$$\omega_{min} = 2\sqrt{\frac{\frac{\gamma_{la}}{w}\left[-\frac{w}{\text{âĎŐ}}\cos\theta_c - \cos(\theta_c+\beta)\right]}{\rho({R_1}^2 - {R_0}^2)}} \quad (15)$$

A similar angular velocity criterion (albeit for a different geometry) is applicable for the capillary valve located at the junction of the transfer fluid channel and the transfer fluid chamber. Two capillary valves of interest are highlighted in Figure 3.

The density of the fluid (the working fluid or the sample fluid) affects the burst angular velocity of the capillary valves as evident from Equation (15); use of heavier fluids leads to lowering of the burst frequency.

5. Experimental

5.1 Microfluidic disc fabrication

Each microfluidic disc is assembled from five layers: three 1.524 mm thick clear acrylic layers and two 0.075 mm double-sided pressure-sensitive adhesive (PSA) layers. The layers of acrylic and PSA are assembled in an alternating order with the acrylic layers on the top and bottom of a disc. Acrylic sheets (McMaster-Carr, USA) are cut by a CO_2 laser cutter (Universal Laser Systems, USA) and the PSA layers (Flexcon, USA) are cut by a standard cutter-plotter (Graphtec America, Japan). The fluidic features are designed using computer aided design software and the drawing files are used as the input for cutting hardware such as the laser cutter. Details of the fabrication process can be found in the article published by (Siegrist et al. 2010).

5.2 Visualization setup

The assembled disc is first loaded with sample fluid (DI water mixed with food coloring) in the sample fluid chamber. It is then spun at 3000 rpm in order to equalize the fluid level in the sample fluid chamber and the transfer channel. It is evident that the acrylic disc is sufficiently hydrophobic as the fluid does not whisk through the channels in the absence of the centrifugal force. Next, the working fluid is loaded in the working fluid chamber and the loading holes are covered with a tape to create the ventless network. The disc operation and visualization are performed on an integrated setup (CD Imager K1000, Key Lead Solutions Inc., USA) that consists of a spinning motor, strobe light, camera and a stereo microscope. This platform offers full synchronization for capturing one frame per revolution of the disc. These images can be studied individually or can be seen as a movie clip (Figure 4).

6. Results and Discussion

A 2D plot for the theoretical hydrostatic pressure head vs. working fluid travel distance (Figure 5) shows that the micro-pulley of the selected design can successfully operate based on the selected fluidic geometry and the selected spin rate (i.e. 650 rpm) as evidenced by the fact that at any point, the sample fluid pressure head is always smaller than the working fluid pressure head. From Figure 5 it can also be seen that there are three distinct regions of pressure head increase and decrease for the sample fluid, corresponding to the three regimes of sample fluid transfer from the sample reservoir through the transfer channel into the transfer chamber. Initially, the sample fluid rise in the transfer channel leads to a sharp increase in the pressure head of the sample fluid; that regime ends when the sample fluid crests the upper bend of the transfer channel and starts flowing into the transfer fluid reservoir. The second regime is gradual emptying of the sample reservoir as the sample fluid is pulled up into the transfer chamber. The sample fluid pressure continues to rise, but much more slowly than in the first regime; that regime ends when the sample fluid reservoir is emptied completely and the sample fluid is left only in the transfer channel between the

bottom of the sample fluid reservoir and the transfer reservoir. The final step, the emptying of the transfer channel itself, similar to the initial step, proceeds very fast as it takes very little travel distance of the working fluid to impose a large displacement of the sample fluid in the transfer channel due to a large difference between the cross-sectional area of the working fluid reservoir and that of the transfer channel (i.e., the ratio of $\frac{A_w}{A_{tr}}$ as seen in Equation (10)).

The three-dimensional plot in Figure 6 expands the 2D graph of the interrelation between the pressure heads of the sample and of the working fluids by adding the dependence on the angular velocity of the disc. Both, the working fluid and the sample pressure heads increase at the same rate, regardless of the angular velocity, as can be seen from Equation (9) where the angular velocity term is the same on both sides of the equation.

The experimental results for micro-pulley operation at 650 rpm confirmed the prediction of our analytical model. The sample fluid level changes are presented in a sequence of images in Figure 7. The movie clip showing the complete fluid transfer process is available as a Supplementary Material on the journal's website.

Even though theoretically there should be no difference for micro-pulley operation for various angular velocities, in practice, there are two limiting factors related to angular velocity that define the operating window for micro-pulley on discs: 1) minimum operating angular velocity is defined by the burst frequency of capillary valves (see Figure 3) discussed above; 2) maximum operating angular velocity is defined by the expansion of the air pocket in the ventless network and it is determined from Equation (8).

According to Equation (15) the capillary valve formed on top of the transfer chamber (Figure 3) has a burst angular velocity of about 430 rpm and the hydrophobic passive valve at the working fluid chamber exit burst at about 240 rpm. Therefore the lower limit for the operating angular velocity is about 430 rpm (45 rad/s). The maximum operating angular velocity for micro-pulley operation calculated from Equation (8) using the specific geometry of our disc (working fluid chamber length of 30 mm, cross-sectional area of the working fluid chamber of 4.6 mm^2, etc.) is predicted to be about 2600 rpm (272 rad/s).

In our experiments we determined that the higher the angular velocity is, the more the working fluid needs to travel to activate the micro-pulley and completely transfer the sample fluid. This indicates that for higher angular velocities, a higher degree of stretching of the air pocket in the ventless network can happen or, there is more air diffusing through the working fluid into the air pocket. In accordance with the predicted maximum operating angular velocity, the fluid transfer by the micro-pulley did not occur on a disc spinning faster than 2600 rpm.

Figure 8 depicts the volume conservation within the ventless network by analyzing the working and sample fluids' level changes. The solid line reflects the theoretical relationship between working and sample fluid travel distances in the corresponding reservoirs given by Equation (11) that assumes no expansion of the air pocket in the ventless network.

Experimental values for working fluid travel on Figure 8 all lay above the theoretical predictions, with the offset that reflects the stretching of the air pocket at 650 rpm.

Therefore, our choice of operating angular velocity of 650 rpm is appropriate as it falls in the micro-pulley's operation range between 450 and 2600 rpm and it is positioned in the lower range of acceptable angular velocities as at higher rpm there is a larger stretching of the air pocket in the ventless network leading to needless loss of the pressure head of the working fluid.

We suggest using a larger volume of working fluid than the minimum value suggested by theoretical calculations above to overcome the additional restraining capillary force present in hydrophobic channels, to account for air pocket stretching and to ensure that manufacturing and materials properties variability do not impede the successful operation of micro-pulleys on a disc. For example, it is suggested that the length of the working fluid chamber be more than twice as long as needed according to theoretical predictions. This design proved to be reproducible and reliable (see supplementary material for the details of the design of specific fluidic features of the micro-pulley disc tested in the presented study).

7. Conclusion

In this study we have demonstrated the design and implementation of fluidic micro-pulleys on centrifugal microfluidic platforms. The micro-pulley can be utilized for fluid transfer on a spinning disc from the outer edge of a disc toward its center. This micro-pulley requires no peripheral components for actuation and is solely driven by the centrifugal force present on rotating platforms. One of the advantageous features of the presented micro-pulley design is a separation of the working fluid from the sample fluid allowed by the use of the non-contact ventless network. Therefore it is possible to use working fluids of various densities to tune the burst frequency of the capillary valve for the disc of a given geometry. Micro-pulleys can also be used sequentially and their action can be designed to start at different angular velocities. In addition to the adjustment of the burst frequencies of capillary valves (that depend on the geometry of the valve and the properties of the working fluid), performance of micro-pulleys can be tailored to various specifications by changing chamber locations and lengths and the level of the fluids in various chambers on micro-pulleys. The possibility of changing a wide variety of parameters for micro-pulley tuning adds a high degree of flexibility and freedom in designing and integrating the micro-pulleys into the complex assays on the microfluidic discs. For instance samples can undergo processes such as lysis and separation at particular angular velocities that do not activate the micro-pulleys. Once the samples are prepared and ready for transfer to another chamber, a higher angular velocity will activate the micro-pulleys. The novel micro-pulley technology executed on hydrophobic microfluidic discs can be employed to more efficiently design complex biological/chemical assays such as immunoassays (Lai et al. 2004) and DNA genotyping (Focke et al. 2010) on the microfluidic discs. As an addition to the existing fluidic toolbox, these micro-pulleys can be combined with other fluidic tools to enhance the fluid flow control on the discs. Figure 9 shows an example of integration that combines the use of active valves (such as wax valves) and micro-pulleys. It is important to notice that in this example the external energy supplied to melt the wax plugs is not used to push the fluid

toward the center of the disc. The energy used for the fluid propulsion toward the disc center is supplied by the potential energy of the working fluid stored on the disc and it is released when the active valves open. The long fluidic path provided in this example can be utilized for complex multi-step assays on the disc in order to accommodate a higher number of steps in a more compact design.

Supplementary Material

Refer to Web version on PubMed Central for supplementary material.

Acknowledgments

The authors would like to thank Sanaz Moslemi-Asl and Alexandra Perebikovsky for their assistance with the graphics and Sheldon Smilo (OmegaTek) for the spinning disc image acquisition / processing. This work was supported by the National Institute of Health grant 1 R01 AI089541-01 and sponsored by WCU (World Class University) program (R32-2008-000-20054-0) through the National Research Foundation of Korea funded by the Ministry of Education, Science and Technology.

References

Abi-Samra K, Clime L, Kong L, Gorkin R, Kim T-H, Cho Y-K, Madou M. Thermo-pneumatic pumping in centrifugal microfluidic platforms. Microfluidics and Nanofluidics. 2011

Becker H, Gärtner C. Polymer microfabrication technologies for microfluidic systems. Analytical and bioanalytical chemistry. 2008; 390(1):89–111. [PubMed: 17989961]

Burtis C, Mailen J, Johnson W, Scott C, Tiffany T, Anderson N. Development of a miniature fast analyzer. Clinical chemistry. 1972; 18(8):753–761. [PubMed: 4339637]

Chen JM, Huang PC, Lin MG. Analysis and experiment of capillary valves for microfluidics on a rotating disk. Microfluidics and Nanofluidics. 2008; 4(5):427–437.

Cho YK, Lee JG, Park JM, Lee BS, Lee Y, Ko C. One-step pathogen specific DNA extraction from whole blood on a centrifugal microfluidic device. Lab Chip. 2007; 7(5):565–573. [PubMed: 17476374]

Ducree J, Haeberle S, Lutz S, Pausch S, von Stetten F, Zengerle R. The centrifugal microfluidic bio-disk platform. J Micromech Microeng. 2007; 17(7):S103–S115.

Focke M, Stumpf F, Roth G, Zengerle R, von Stetten F. Centrifugal microfluidic system for primary amplification and secondary real-time PCR. Lab Chip. 2010; 10(23):3210–3212. [PubMed: 20938554]

Garcia-Cordero JL, Basabe-Desmonts L, Ducree J, Ricco AJ. Liquid recirculation in microfluidic channels by the interplay of capillary and centrifugal forces. Microfluidics and Nanofluidics. 2010; 9(4–5):695–703.

Gorkin R, Clime L, Madou M, Kido H. Pneumatic pumping in centrifugal microfluidic platforms. Microfluidics and Nanofluidics. 2010a; 9(2–3):541–549.

Gorkin R, Nwankire CE, Gaughran J, Zhang X, Donohoe GG, Rook M, O'Kennedy R, Ducree J. Centrifugo-pneumatic valving utilizing dissolvable films. Lab Chip. 2012a; 12(16):2894–2902. [PubMed: 22692574]

Gorkin R, Park J, Siegrist J, Amasia M, Lee BS, Park J-M, Kim J, Kim H, Madou M, Cho Y-K. Centrifugal microfluidics for biomedical applications. Lab Chip. 2010b; 10:1758–1773. [PubMed: 20512178]

Gorkin R, Soroori S, Southard W, Clime L, Veres T, Kido H, Kulinsky L, Madou M. Suction-enhanced siphon valves for centrifugal microfluidic platforms. Microfluidics and Nanofluidics. 2012b; 12(1–4):345–354.

Grumann M, Geipel A, Riegger L, Zengerle R, Ducree J. Batch-mode mixing on centrifugal microfluidic platforms. Lab Chip. 2005; 5(5):560–565. [PubMed: 15856095]

Haeberle S, Zengerle R. Microfluidic platforms for lab-on-a-chip applications. Lab on a Chip. 2007; 7(9):1094–1110. [PubMed: 17713606]

Kazarine A, Kong MC, Templeton EJ, Salin ED. Automated Liquid–Liquid Extraction by Pneumatic Recirculation on a Centrifugal Microfluidic Platform. Analytical chemistry. 2012; 84(16):6939–6943. [PubMed: 22845877]

Kido H, Micic M, Smith D, Zoval J, Norton J, Madou M. A novel, compact disk-like centrifugal microfluidics system for cell lysis and sample homogenization. Colloid Surface B. 2007; 58(1): 44–51.

Kirby D, Siegrist J, Kijanka G, Zavattoni L, Sheils O, O'Leary J, Burger R, Ducrée J. Centrifugo-magnetophoretic particle separation. Microfluidics and Nanofluidics. 2012:1–10.

Kong MC, Bouchard AP, Salin ED. Displacement Pumping of Liquids Radially Inward on Centrifugal Microfluidic Platforms in Motion. Micromachines. 2011; 3(1):1–9.

Kong MC, Salin ED. Pneumatically pumping fluids radially inward on centrifugal microfluidic platforms in motion. Analytical chemistry. 2010; 82(19):8039–8041. [PubMed: 20815346]

Lai S, Wang S, Luo J, Lee LJ, Yang S-T, Madou MJ. Design of a compact disk-like microfluidic platform for enzyme-linked immunosorbent assay. Analytical chemistry. 2004; 76(7):1832–1837. [PubMed: 15053640]

Li C, Dong X, Qin J, Lin B. Rapid nanoliter DNA hybridization based on reciprocating flow on a compact disk microfluidic device. Analytica chimica acta. 2009; 640(1):93–99. [PubMed: 19362626]

Love LJ, Jansen JF, McKnight TE, Roh Y, Phelps TJ. A magnetocaloric pump for microfluidic applications. NanoBioscience, IEEE Transactions on. 2004; 3(2):101–110.

Madou M, Zoval J, Jia GY, Kido H, Kim J, Kim N. Lab on a CD. Annu Rev Biomed Eng. 2006; 8:601–628. [PubMed: 16834568]

Madou, MJ. Fundamentals of microfabrication : the science of miniaturization. 2nd edn.. Boca Raton: CRC Press; 2002.

Madou MJ, Lu Y, Lai S, Koh CG, Lee LJ, Wenner BR. A novel design on a CD disc for 2-point calibration measurement. Sensors and Actuators-A-Physical Sensors. 2001; 91(3):301–306.

Mark D, van Oordt T, Strohmeier O, Roth G, Drexler J, Eberhard M, Niedrig M, Patel P, Zgaga-Griesz A, Bessler W, Weidmann M, Hufert F, Zengerle R, von Stetten F. Automated and miniaturized detection of biological threats with a centrifugal microfluidic system. SPIE. 2012; 8367

Noroozi Z, Kido H, Madou MJ. Electrolysis-Induced Pneumatic Pressure for Control of Liquids in a Centrifugal System. Journal of The Electrochemical Society. 2011; 158(11):P130–P135.

Siegrist J, Gorkin R, Clime L, Roy E, Peytavi R, Kido H, Bergeron M, Veres T, Madou M. Serial siphon valving for centrifugal microfluidic platforms. Microfluidics and Nanofluidics. 2010; 9(1): 55–63.

Steigert J, Grumann M, Brenner T, Riegger L, Harter J, Zengerle R, Ducrée J. Fully integrated whole blood testing by real-time absorption measurement on a centrifugal platform. Lab Chip. 2006; 6:1040–1044. [PubMed: 16874375]

Thio THG, Ibrahim F, Al-Faqheri W, Moebius J, Khalid NS, Soin N, Kahar MKBA, Madou MJ. Push pull microfluidics on a multi-level 3D CD. Lab Chip. 2013

Tsao CW, DeVoe DL. Bonding of thermoplastic polymer microfluidics. Microfluidics and Nanofluidics. 2009; 6(1):1–16.

Zehnle S, Schwemmer F, Roth G, Von Stetten F, Zengerle R, Paust N. Centrifugo-dynamic inward pumping of liquids on a centrifugal microfluidic platform. Lab Chip. 2012; 12(24):5142–5145. [PubMed: 23108455]

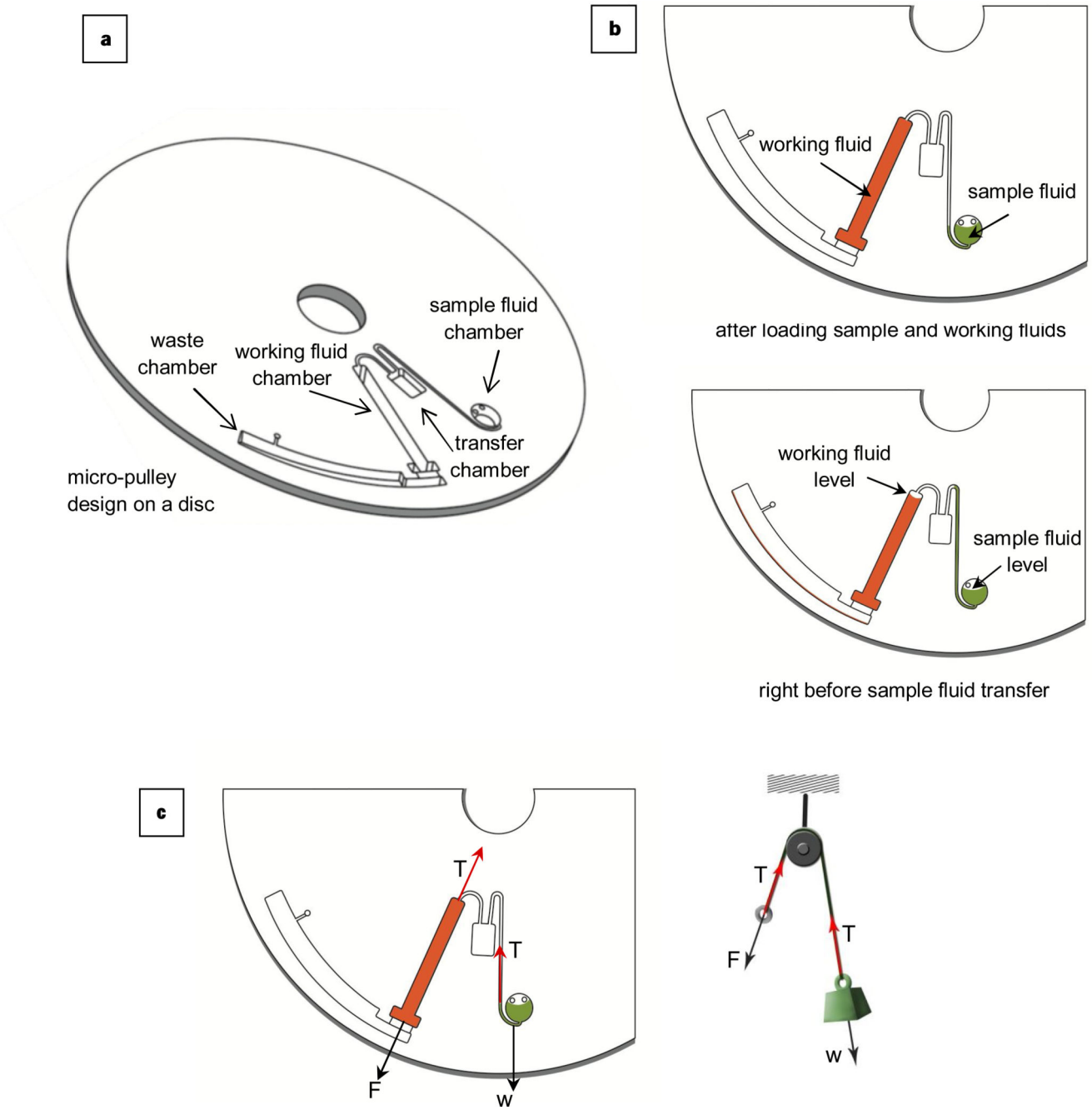

Figure 1.

a) Schematic design of a centrifugal micro-pulley system, b) fluid transfer mechanism of the centrifugal “micro-pulley” system, c) analogy of the “micro-pulley” fluidic system to a simple pulley

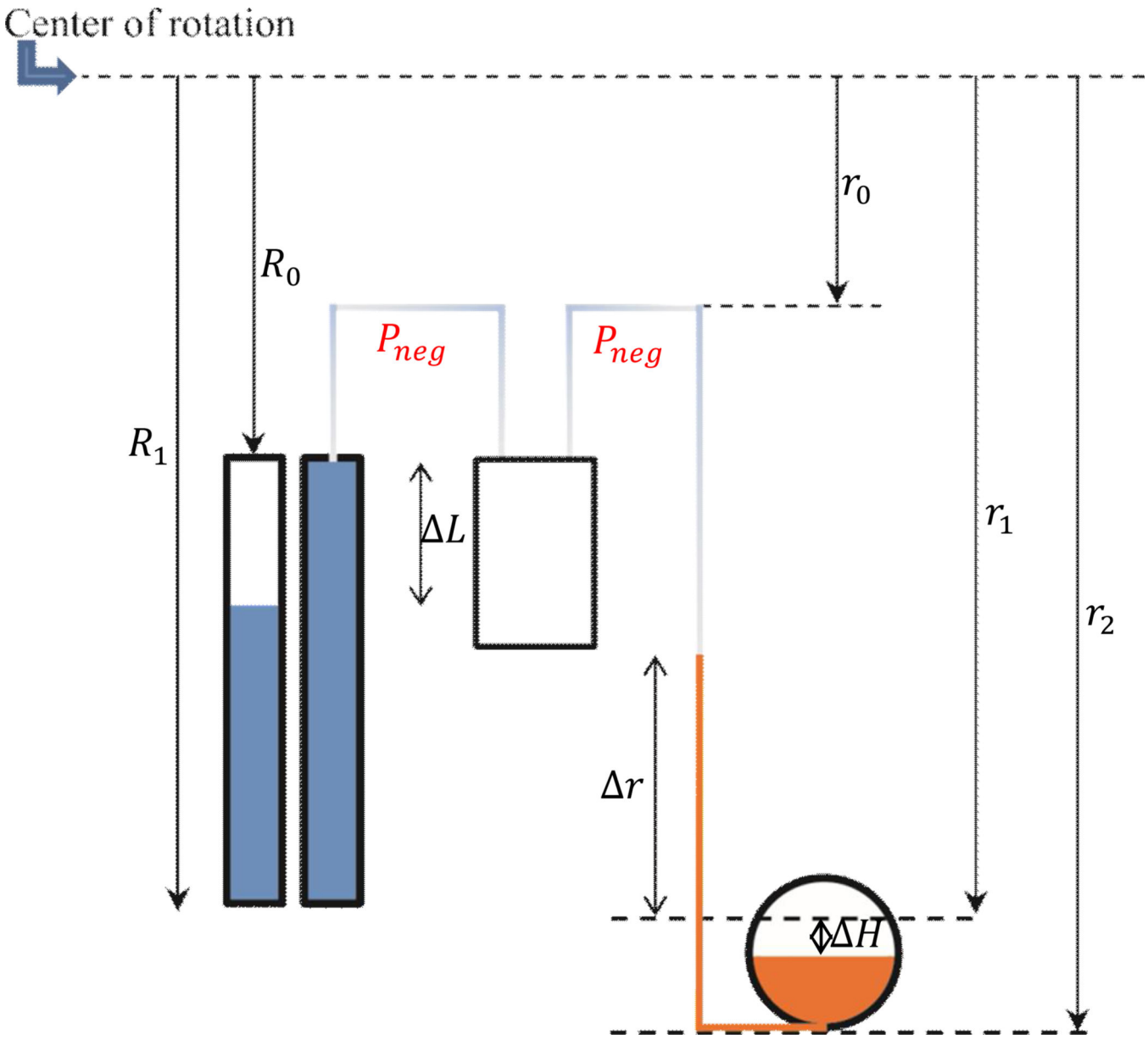

Figure 2.
The geometry of the centrifugal micro-pulley system (see Section 3.2 for explanation of the variables)

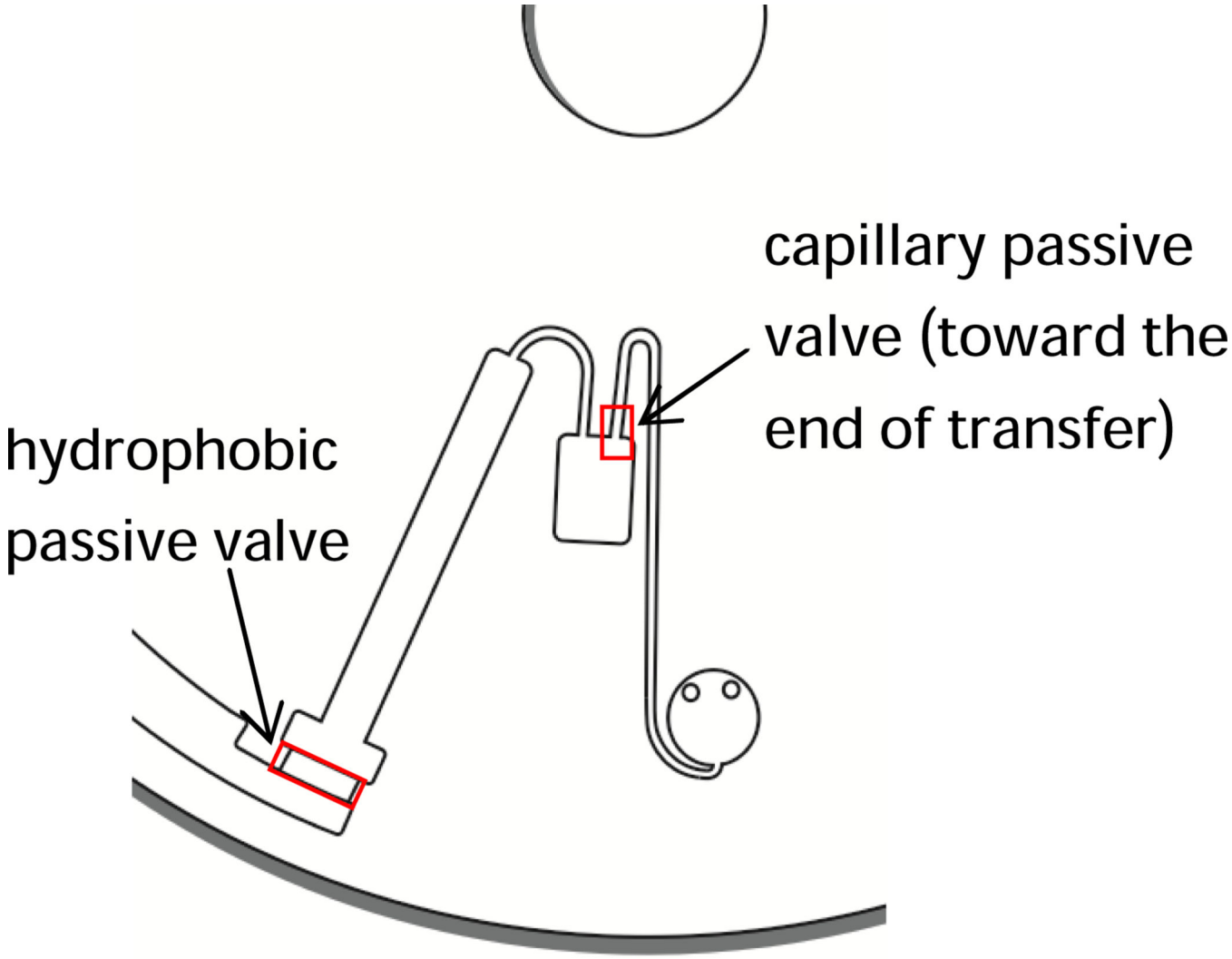

Figure 3.
Hydrophobic and capillary valves embedded in the centrifugal micro-pulley system

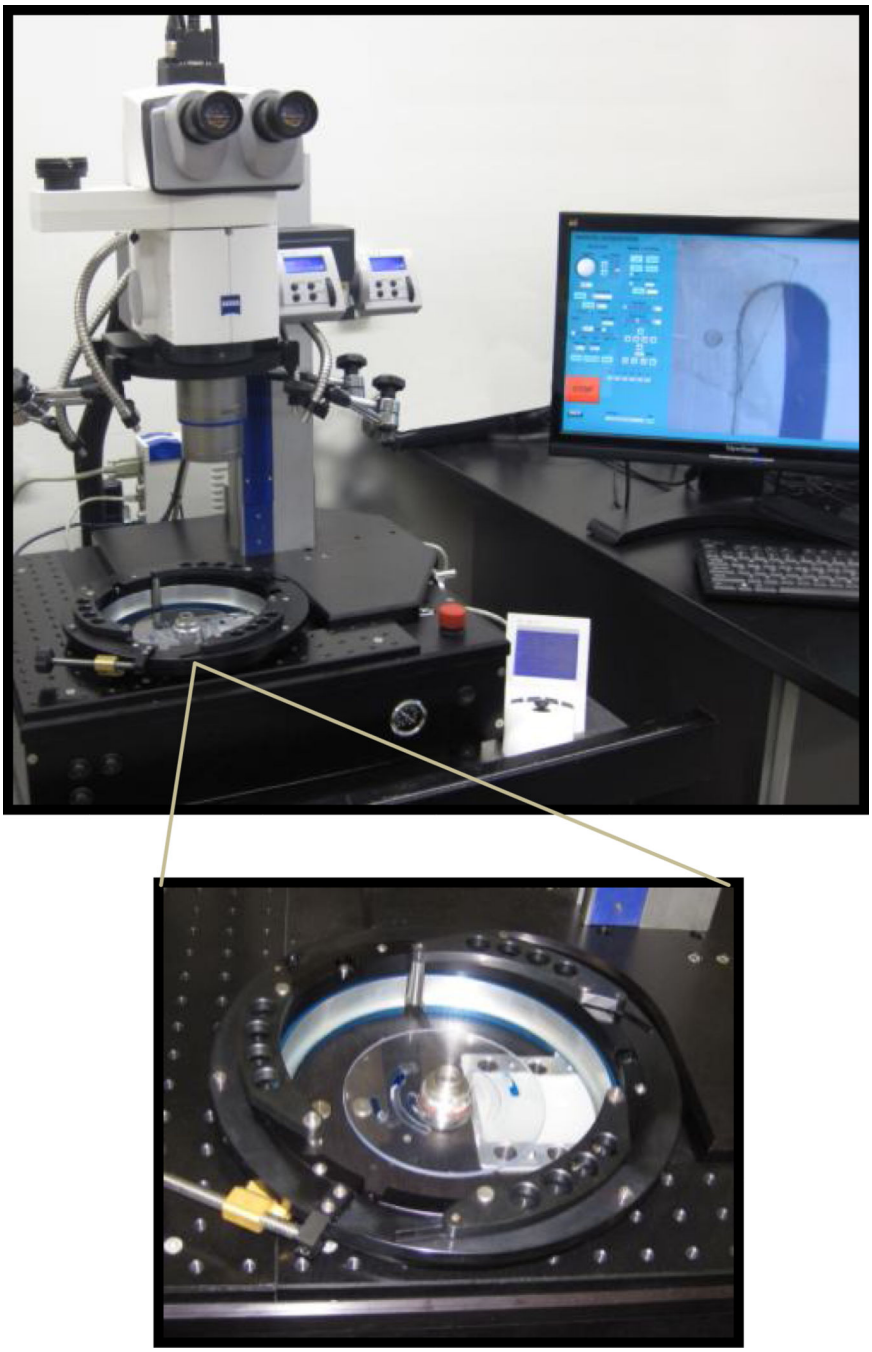

Figure 4.
CD Imager K1000 used for image acquisition of spinning discs

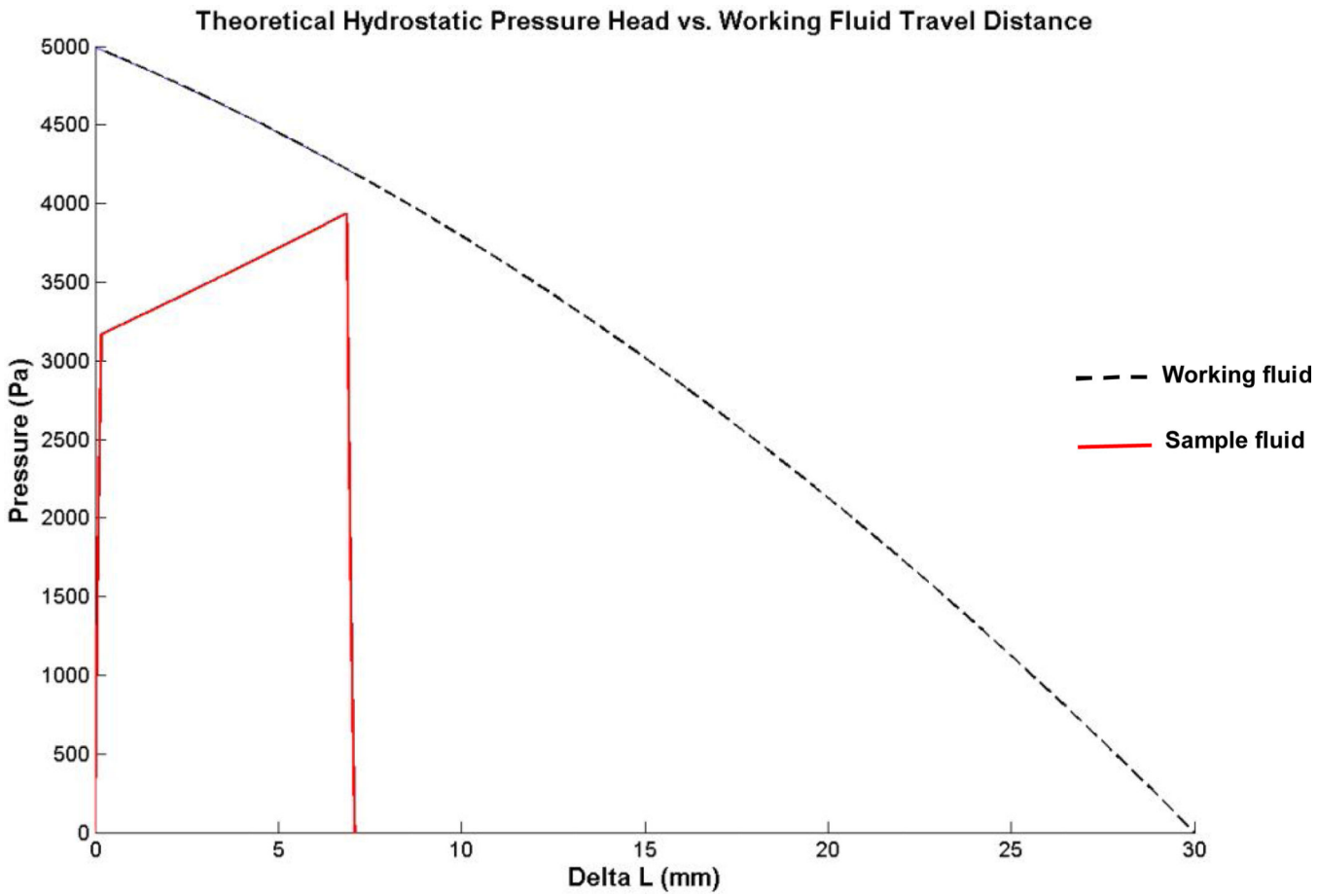

Figure 5.

The plot for hydrostatic pressure head for working and sample fluids vs. working fluid travel distance. This plot shows that the sample fluid pressure head never reaches the working fluid pressure head and therefore the sample fluid can be successfully transferred into the upstream transfer fluid reservoir.

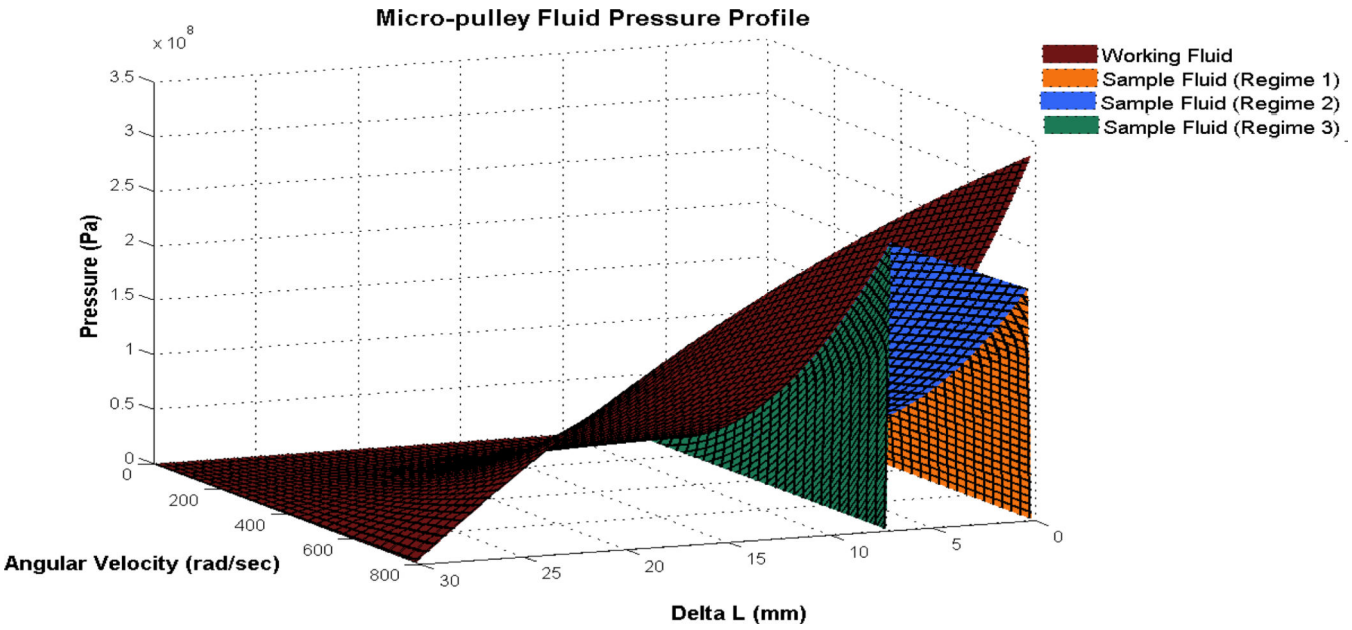

Figure 6.

Relationship between hydrostatic heads of the sample and working fluids with respect to the travel distance of the working fluid and the operating angular velocity of the disc. The details of disc design are given in the Supplementary Materials section.

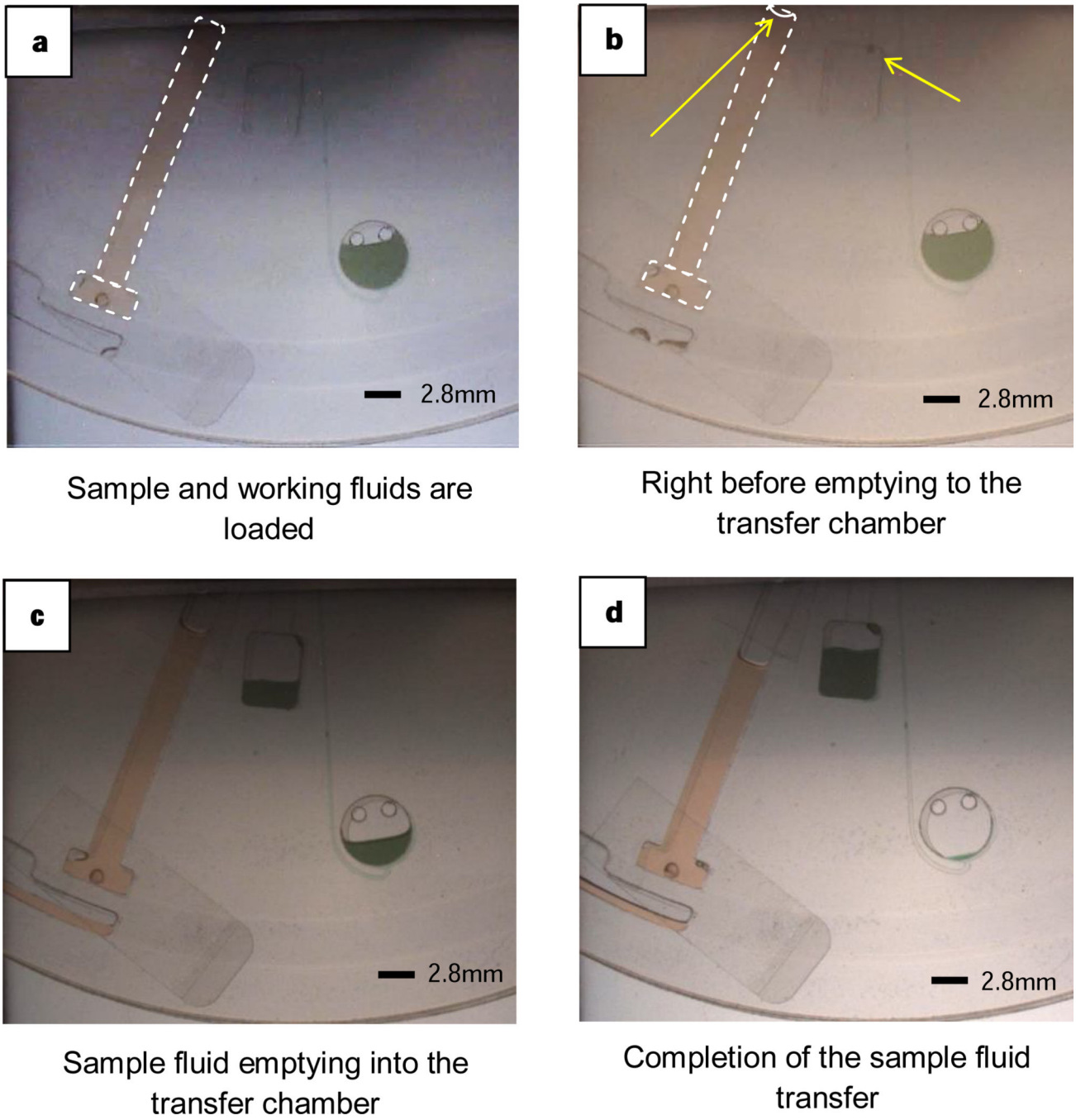

Figure 7.

Sample fluid transfer process: a) the working fluid and the sample fluid chambers are loaded (the working fluid chamber is indicated by the dashed lines and the chamber is fully loaded with the working fluid), b) right before the transfer of the sample fluid from the transfer channel to the transfer chamber (the working fluid chamber is indicated by the dashed lines, the working fluid meniscus level is shown by the curved white line; left arrow pointing to it, the right arrow points to the first drop of the sample fluid that is about to enter the transfer

chamber), c) during the sample fluid transfer, and d) completion of the transfer right before the last drop of the sample fluid goes into the transfer chamber.

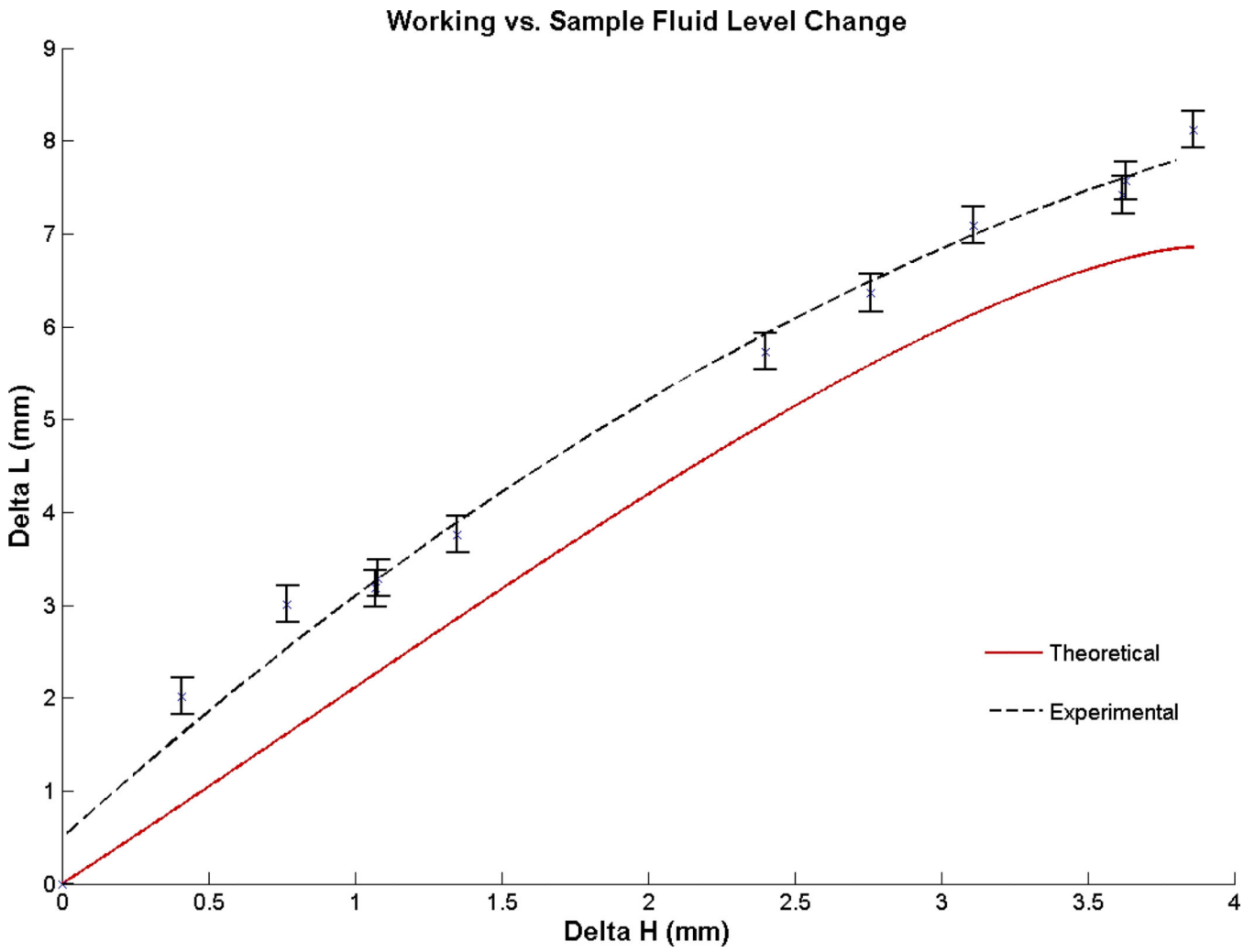

Figure 8.

The plot of relationship between the change in levels of working and sample fluids in their respective reservoirs. Experimental data confirms the stretching of the air pocket in the ventless network. The error bars show ±0.5 mm due to limitations in distance measurements smaller than 0.5 mm.

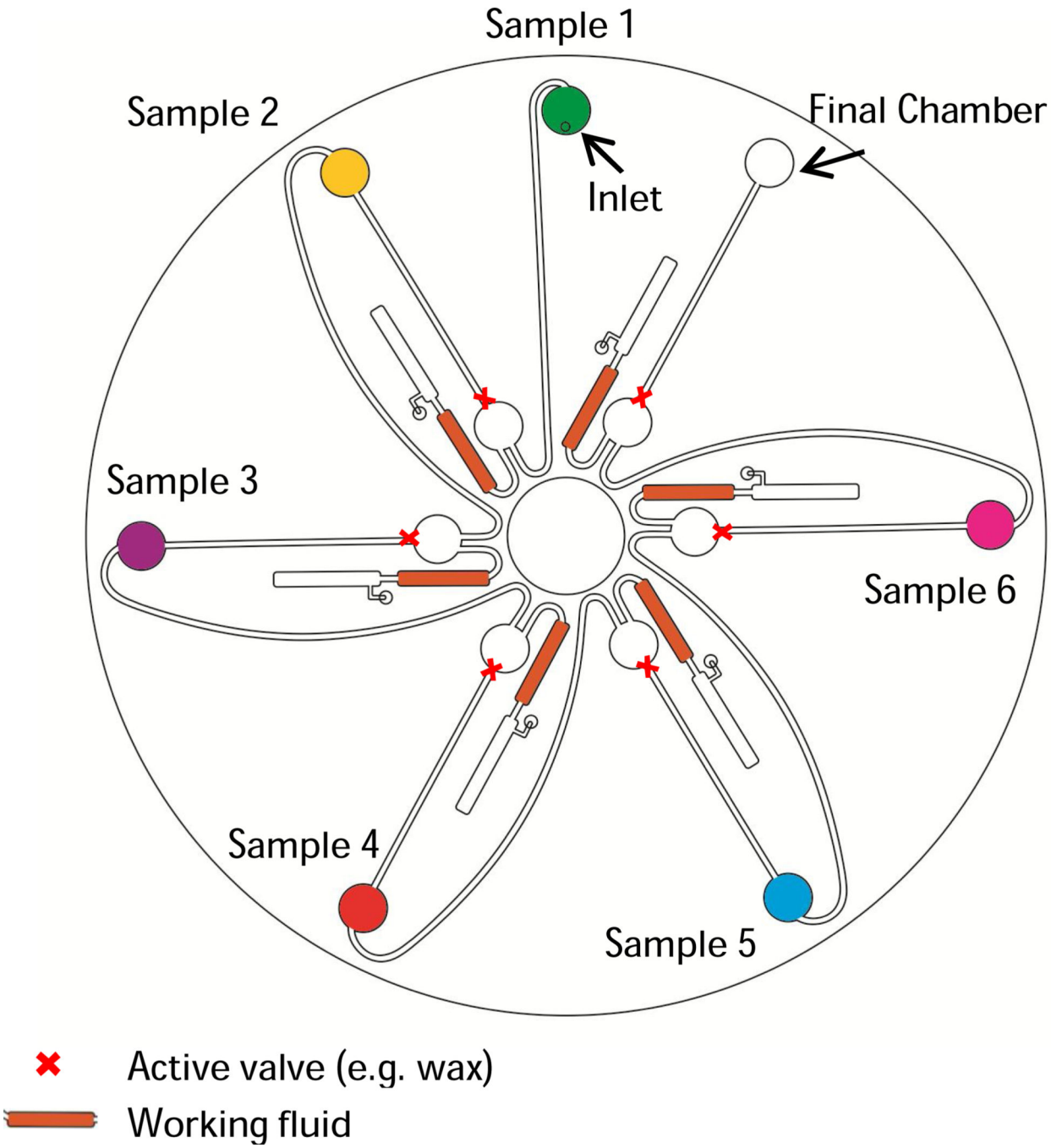

Figure 9.
Schematic design of integrated micro-pulleys with active wax valves for implementation of complex multi-step biological and chemical assays on discs